Empirical Wavelet Transform Based Method for Identification and Analysis of Sub-synchronous Oscillation Modes Using PMU Data

Joice G. Philip, Jaesung Jung, *Member*, *IEEE*, and Ahmet Onen

***Abstract*—This paper proposes an empirical wavelet transform (EWT) based method for identification and analysis of sub-synchronous oscillation (SSO) modes in the power system using phasor measurement unit (PMU) data. The phasors from PMUs are preprocessed to check for the presence of oscillations. If the presence is established, the signal is decomposed using EWT and the parameters of the mono-components are estimated through Yoshida algorithm. The superiority of the proposed method is tested using test signals with known parameters and simulated using actual SSO signals from the Hami Power Grid in Northwest China. Results show the effectiveness of the proposed EWT-Yoshida method in detecting the SSO and estimating its parameters.**

***Index Terms*—Empirical wavelet transform (EWT), sub-synchronous oscillation, Prony-based method, Yoshida algorithm, variational mode decomposition, phasor measurement unit (PMU).**

I. Introduction

SUB-SYNCHRONOUS oscillation (SSO) are one of the biggest threats affecting the stability and security of power systems. In conventional power systems, SSOs occur owing to the interaction among the mechanical system of the generator and series compensated lines, high-voltage direct current (HVDC) controls or flexible alternative current transmission system (FACTS) devices [1]. With the penetration of renewable energy resources such as wind turbine generators (WTGs), SSOs are being increasingly observed in renewable energy integrated power systems. The main reason for their occurrence is the interaction between the converter controls of the WTG with the series compensated lines or the weak AC grid. This phenomenon is known as sub-synchronous control interaction (SSCI). The first reported SSCI incident was recorded in Electric Reliability Council of Texas (ERCOT), Texas, USA, in 2009 [2]. Similar SSCI incidents also occurred in Xcel Energy Network, Minnesota USA [3], Guyam Power System, China [4], and other parts of the world. The persistence of these oscillations in power system endangers its regular operation and may even cause blackouts. Hence, it is essential to identify these oscillations and implement corrective measures at the earliest.

The states of the modern power systems are mainly monitored through phase measurement unit (PMU) based wide area measurement systems (WAMSs) [5]-[7]. Therefore, several measurement based methods for SSO analysis using PMU data have already been proposed in the literature. They are broadly divided into time-domain, frequency-domain, and time-frequency-domain based methods [8].

Time-domain based methods such as estimation of signal parameters via rotational invariance techniques (ESPRITs) [9], [10], dynamic mode decomposition (DMD) [11], and matrix pencil [12] model the signal as the sum of exponentially decaying sinusoids. In [10], an ESPRIT based method is used for identifying the modal parameters of SSO in the power system. As ESPRIT is a parametric method, it requires an accurate estimate of the model order for its proper operation. This is obtained using the exact model order method. DMD is used in [11] to identify the modal parameters of SSO. In this method, the DMD estimates the eigenvalues and eigenvectors of the signal under consideration, and the modal parameters are calculated from these estimated values. The time-domain based methods generally exhibit satisfactory performance if the model order is correctly pre-determined and the signal-to-noise ratio (SNR) is high.

Frequency-domain based methods mainly use the Fourier transform to estimate the SSO parameters. In [13], [14], an interpolated discrete Fourier transform is used to determine the frequency, damping factor, and amplitude of the SSO. The estimation of modal parameters using improved Yoshida and Bertocco algorithms is proposed in [15]. However, Fourier transform based methods usually have issues related to spectral leakage and the picket fencing effect which limit

Manuscript received: January 28, 2023; revised: June 13, 2023; accepted: August 17, 2023. Date of CrossCheck: August 17, 2023. Date of online publication: November 29, 2023.

This work was supported by Korea Electric Power Corporation (No. R21XO01-38) and Korea Ministry of Environment (MOE) as Graduate School specialized in Climate Change.

The authors thank Mr. Ajinkya Sonawane, Research Scholar, Indian Institute of Technology (IIT), Indore, India, for helping with the simulations of SSO signals.

J. G. Philip is with the Department of Energy Systems Research, Ajou University, Suwon, South Korea (e-mail: joice.philip@hotmail.com).

J. Jung (corresponding author) is with the Department of Energy Systems Research, Ajou University, Suwon, South Korea (e-mail: jjung@ajou.ac.kr).

A. Onen is with the Department of Electrical and Electronic Engineering, Abdullah Gul University, Kayseri, 38080, Turkey, and he is also with the Department of Electrical and Computer Engineering, College of Engineering, Sultan Qaboos University, Al-Khoud, Muscat, Oman (e-mail: a.onen@squ.edu.om).

DOI: 10.35833/MPCE.2023.000047

their application in larger practical systems.

The analysis of SSOs using time-frequency-domain based methods such as variational mode decomposition (VMD), multi-synchrosqeezing transform, and Taylor Fourier transform is proposed in [8], [16]-[18]. VMD-based methods are proposed in [16], [17]. In [17], a VMD-Hilbert method is used for estimating the parameters of the SSO. In this method, the signal is decomposed into mono-components using VMD, and Hilbert's transform is used to identify the frequency and damping factor of the mono-component signals. The detection of SSO modes and their parameter identification using the multi-synchrosqueezing transform is proposed in [8]. Reference [18] uses Taylor Fourier transform for SSO detection and monitoring.

It is observed that the majority of the drawbacks of the time-domain and frequency-domain based methods such as accurate predetermination of model order, spectral leakage, and poor performance under noise contamination are neither present nor as prevalent as in the time-frequency-domain based methods, making them a better option for analyzing power system signals. Wavelet transform based methods are among the most commonly used time-frequency techniques which find applications in areas ranging from signal processing to power systems. However, apart from a few wavelet transform based methods like empirical wavelet transform (EWT) [19], prior information is essential for the proper operation of most wavelet transform based methods. Hence, this paper proposes an EWT-based method for analyzing the SSO in the power system. This method decomposes the multi-frequency signal into single-frequency components using EWT-based filter banks. Furthermore, the frequency and damping factors of these components are calculated using Yoshida algorithm [20]. The novelty of the proposed method are as follows.

1) A preprocessing algorithm based on Welch's power spectral density (WPSD) estimate for the detection of oscillation modes in the power system signal is included in the proposed method to reduce its computational complexity. If the WPSD algorithm detects oscillation modes in the signal, it is further analyzed using EWT-based method. Otherwise, the present signal is discarded and the next set of signal samples is analysed. To the best of authors' knowledge, the analysis of power system oscillations using EWT is proposed in few literature like [21]. Further, a combination of WPSD algorithm and EWT-Yoshida based modal parameter estimation is not proposed in any other research works.

2) The proposed EWT-based method can effectively analyze non-stationary signals. Hence, it can also be used for analyzing SSO occurring owing to SSCI where the frequency of the signal changes with time [22].

3) EWT uses adaptive filters, namely, the wavelets are designed based on the signal information unlike other wavelet methods like discrete wavelet transform (DWT) where conventional wavelets like Morlet and Haar wavelet are used.

The efficacy of the proposed EWT-Yoshida method is tested with two similar signal processing methods based on VMD [17] and Prony [23] using synthetic signals and SSO signals from the Hami Power Grid in Northwest China. The results show the effectiveness of the proposed EWT-Yoshida method in detecting the SSO and estimating its parameters.

II. Methodology

The proposed EWT-Yoshida method is illustrated in Fig. 1. In this method, the signal is decomposed into single-frequency components using EWT. Further, the parameters of these components, namely the frequency f_n and damping factor α_n, are calculated using Yoshida algorithm. As the occurrence of SSO is rare in the power system, a preprocessing algorithm based on the WPSD estimate for detecting the oscillation modes in the signal under consideration is also included in the proposed method. If SSOs are detected, the signal is fed into the EWT-based method for further analysis. Otherwise, the next set of signal samples is considered. The following subsections give a detailed description of the components of the proposed method.

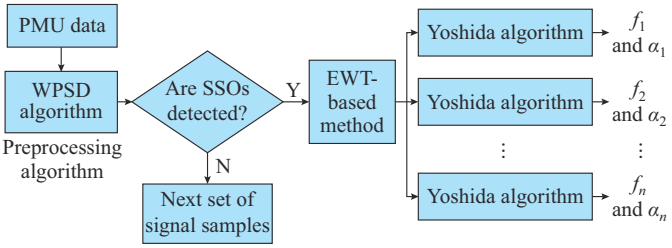

Fig. 1. Proposed EWT-Yoshida method.

A. Preprocessing Algorithm

SSO is a phenomenon that rarely occurs in the power system although the rate of its occurrence has increased in recent years. The proposed method effectively detects and estimates the parameters of the SSO using an algorithm based on EWT-Yoshida method. However, the proposed method can be made simpler if only the signals in oscillation modes are analyzed using the EWT-Yoshida method. Therefore, a preprocessing algorithm for detecting the oscillation modes in the signal is also included in the proposed method. This algorithm utilizes the WPSD estimate to detect the oscillation modes in the signal. If the oscillation modes are detected, the signal is fed into the EWT-based method for further analysis. Otherwise, the next set of samples is analyzed. The details of WPSD algorithm are as follows.

As mentioned above, the proposed EWT-based method uses the WPSD algorithm to detect oscillation modes in the power system signal under consideration. A signal with oscillation modes will have single or multiple peaks in its WPSD plot depending on the number of frequency components in it. The WPSD plot of the signal is obtained using the following equations.

$$S_x(f) = \frac{1}{T}\sum_{t=1}^{T} P_t(f) \tag{1}$$

$$P_t(f) = \frac{1}{W}\left|X_t(f)\right|^2 \tag{2}$$

$$W = \sum_{m=0}^{M} w^2(m) \tag{3}$$

$$X_t(f)=\sum_m x(m)w(m)\mathrm{e}^{-2\pi fm} \tag{4}$$

where $S_x(f)$ is the WPSD estimate; $x(m)$, $w(m)$, and $X_t(f)$ are the signal data, window function, and windowed discrete Fourier transform, respectively; W represents the power of its window function; and T and M represent the lengths of the $P_t(f)$ and $w(m)$, respectively.

Figure 2(a) and (b) shows a single-mode signal with a SNR of 10 dB and its WPSD estimate. It is observed from Fig. 2(b) that the WPSD estimate has one peak corresponding to the single mode in the signal. Similarly, the WPSD estimate of a four-mode signal has four peaks as shown in Fig. 2(d). Therefore, it can be inferred that the WPSD estimate is an excellent choice for identifying signals with oscillation modes [24].

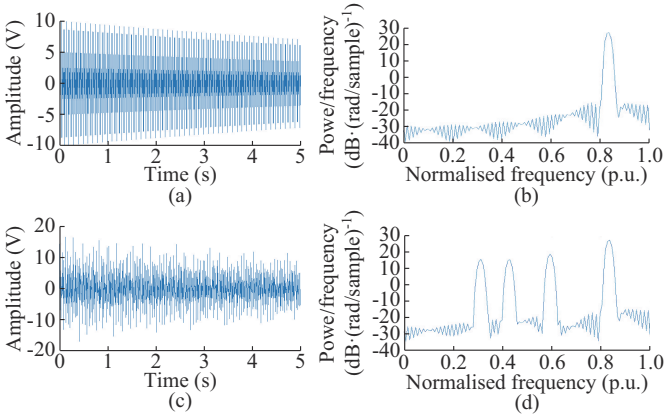

Fig. 2. Signals and their WPSD estimates. (a) Single-mode signal. (b) WPSD estimate of a single-mode signal. (c) Four-mode signal. (d) WPSD estimate of a four-mode signal.

B. EWT

The steps for calculating EWT of the signal is as follows.

Step 1: let $Z(w)$ be the Fourier transform of the signal from PMUs.

Step 2: identify the peaks $(w_1, w_2, ..., w_M)$ of $Z(w)$ with magnitude more than at least 10% of the highest peak. The dominant frequencies of the signal correspond to these peaks.

Step 3: identify the local minima between consecutive peaks. They form the boundaries to split the Fourier spectrum $Z(w)$.

Step 4: create the empirical wavelets $\phi_1(w)$ and $\psi_i(w)$ as shown below.

$$\phi_1(w)=\begin{cases}1 & |w|\le(1-\gamma)\rho_1\\ \cos\left(\dfrac{\pi}{2}\beta(\gamma,w,\rho_1)\right) & (1-\gamma)\rho_1\le|w|\le(1+\gamma)\rho_1\\ 0 & \text{otherwise}\end{cases} \tag{5}$$

$$\psi_i(w)=\begin{cases}1 & (1+\gamma)\rho_i\le|w|\le(1+\gamma)\rho_{i+1}\\ \cos\left(\dfrac{\pi}{2}\beta(\gamma,w,\rho_{i+1})\right) & (1-\gamma)\rho_{i+1}\le|w|\le(1+\gamma)\rho_{i+1}\\ \sin\left(\dfrac{\pi}{2}\beta(\gamma,w,\rho_i)\right) & (1-\gamma)\rho_i\le|w|\le(1+\gamma)\rho_i\\ 0 & \text{otherwise}\end{cases} \tag{6}$$

$$\beta(\gamma,w,\rho_i)=\beta\left\{\frac{1}{2\gamma\rho_i}\left[|w|-(1-\gamma)\rho_i\right]\right\} \tag{7}$$

where ρ_i and γ are the boundary between the consecutive peaks and parameter for overlap prevention between two consecutive transition areas, respectively. Sine and cosine functions are fitted by an arbitrary function $\beta(\gamma,w,\rho_i)$.

Step 5: calculate the detail and approximate coefficients of the signal as:

$$EWT(1,n)=IFFT(Z(w)\phi_1(w)) \tag{8}$$

$$EWT(i,n)=IFFT(Z(w)\psi_i(w)) \tag{9}$$

where *IFFT* is the inverse fast fourier transform (FFT) of the signal.

The decomposed mono-component signals are present in $EWT(1,n)$ and $EWT(i,n)$. The superiority of EWT in decomposing multi-mode signals into its mono-components can be illustrated by the following example.

As shown below, let $z(t)$ be a two-mode signal.

$$z(t)=10\mathrm{e}^{-0.15t}\sin(2\pi\times10t)+3\mathrm{e}^{-0.15t}\sin(2\pi\times20t) \tag{10}$$

The FFT spectrum of $z(t)$ is shown in Fig. 3(b). It is observed that $z(t)$ contains two dominant modes with frequencies of 10 Hz and 20 Hz. The local minima between these frequencies form the boundary for splitting the FFT spectrum, as shown in Fig. 3(b). Empirical wavelets are designed based on these boundaries, and the signal $z(t)$ is later split into its mono-components using these wavelets. The decomposed mono-components of $z(t)$ are shown in Fig. 3(c) and (d) [19].

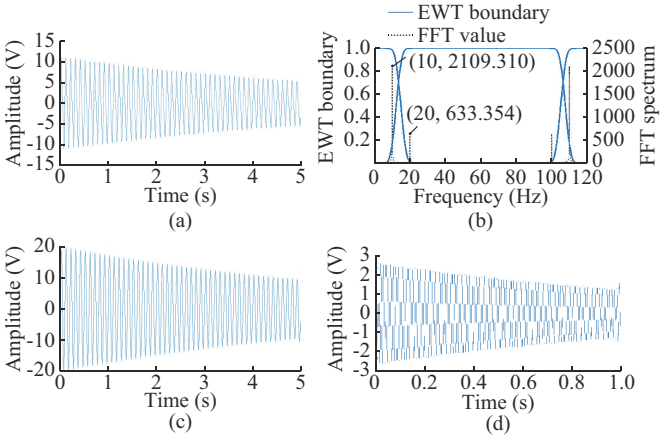

Fig. 3. Signal $z(t)$ and its mono-components. (a) Signal $z(t)$. (b) FFT spectrum and EWT boundaries. (c) 10 Hz mode. (d) 20 Hz mode.

C. Yoshida Algorithm

The mono-components obtained from the output of the EWT-based filter bank are fed into Yoshida algorithm which is used to obtain its frequency and damping factor. The major steps of this algorithm are as follows.

Step 1: plot the FFT of the mono-component signal and determine its peaks. Let the FFT of the mono-component be Z_w and its peak occurs at p_n.

Step 2: find the ratio R using the following equation:

$$R=\frac{Z_w(p_1)-2Z_w(p_2)+Z_w(p_3)}{Z_w(p_2)-2Z_w(p_3)+Z_w(p_4)} \tag{11}$$

where $[p_1,p_2,p_3,p_4]=[p_{n-1},p_n,p_{n+1},p_{n+2}]$ when $Z_w(p_n+2)\geq Z_w(p_n-2)$; and $[p_1,p_2,p_3,p_4]=[p_{n+1},p_n,p_{n-1},p_{n-2}]$ when $Z_w(p_n+2)<Z_w(p_n-2)$.

Step 3: estimate the frequency f_i and damping factor ζ_i of the mono-components using the following equations.

$$f_i=\begin{cases}\dfrac{f_s}{N}\cdot\mathrm{Re}\left(p_n-1-\dfrac{3}{R-1}\right) & Z_w(p_n+2)\geq Z_w(p_n-2)\\ \dfrac{f_s}{N}\cdot\mathrm{Re}\left(p_n-2-\dfrac{3}{R-1}\right) & Z_w(p_n+2)<Z_w(p_n-2)\end{cases} \tag{12}$$

$$\zeta_i=\frac{f_s}{N}\cdot\mathrm{Im}\left(\frac{3}{R-1}\right) \tag{13}$$

where f_s and N are the sampling frequency and length of the mono-component, respectively [13], [20].

The effectiveness of the Yoshida algorithm is proven using the mono-components of $z(t)$ given in Section II-B.

Table I lists the true and estimated values of $z(t)$. It is observed that the Yoshida algorithm provides accurate estimates of the frequency and damping factor of the modes of $z(t)$, proving their effectiveness.

TABLE I
TRUE AND ESTIMATED VALUES OF $z(t)$

Mode	True value		Estimated value	
	Frequency	Damping factor	Frequency	Damping factor
Mode 1	10	–0.15	10	–0.1499
Mode 2	20	–0.15	20	–0.1488

III. SIMULATION RESULTS AND DISCUSSION

The performance of the proposed EWT-Yoshida method is tested using test signals with known parameters and SSO signal from Hami Power Grid in Northwest China [25]. The simulations are conducted using MATLAB 2021. x with a workstation with Intel Core i5-10th Gen processor and 8 GB of RAM.

A. Test Signals

Two signals, i. e., $x(t)=A_1e^{-\zeta_1 t}\sin(2\pi f_1 t)+A_s e^{-\zeta_s t}\sin(2\pi f_{ss}t)$ and $y(t)=4e^{-0.16t}\sin(2\pi\cdot 1.71t)+2e^{-0.15t}\sin(2\pi\cdot 12.67t)+2e^{-0.14t}\cdot\sin(2\pi\cdot 19.62t)$ are used to test the robustness of the proposed method, where A_1, f_1, ζ_1, A_s, f_{ss}, ζ_s are the parameters of $x(t)$. These signals are sampled at 50 Hz which is one of the PMU reporting rates specified in [23].

1) Case study 1: frequency variation. The robustness of the proposed method against the change in the frequency of the SSO mode is tested using $x(t)$ in this case study.

The frequency of the SSO mode varies from 19.5 Hz to 38.5 Hz in steps of 1 Hz, as shown in Table II, and the parameters of the resulting signals are estimated for this purpose.

TABLE II
PARAMETERS OF $x(t)$ FOR CASE STUDY 1

A_1	f_1 (Hz)	ζ_1	A_s	f_{ss} (Hz)	ζ_s
10	1.22	–0.07	3	[19.5, 38.5]	–0.05

Figures 4 and 5 show the WPSD estimate of $x(t)$ and estimation errors of frequency and damping factor for the above case. It is noticed that the estimated values of the parameters are almost similar to the true ones. The maximum errors in estimating the frequency and damping factors are 0.005% and 1.4%, respectively. It is also observed that the estimation error of parameter is almost constant irrespective of the frequency of SSO mode. This proves that the proposed method provides accurate parameter estimates irrespective of the frequency of the modes of the signal.

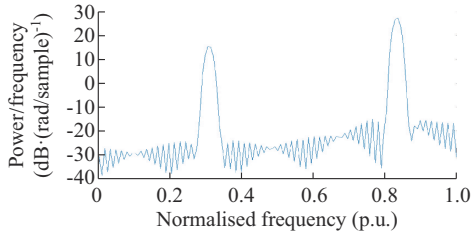

Fig. 4. WPSD estimate of $x(t)$ with $f_{ss}=19.5$ Hz.

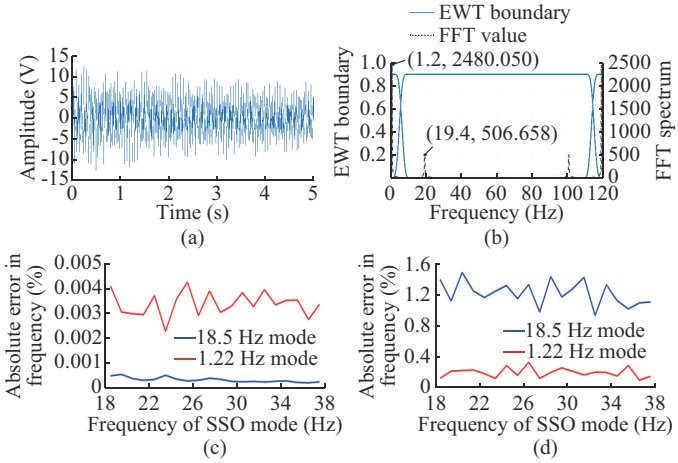

Fig. 5. Estimation errors of parameters of $x(t)$ when frequency of SSO mode varies from 19.5 Hz to 38.5 Hz. (a) $x(t)$. (b) FFT of $x(t)$ with EWT boundaries. (c) Estimation error of frequency. (d) Estimation error of damping factor.

2) Case study 2: damping factor variation. The effectiveness of the proposed method against variations in the damping factor of the SSO mode is investigated in this case study using $x(t)$. The damping factor of the SSO mode varies from –0.24 to –0.05 in steps of –0.01 Hz, as shown in Table III, and the parameters of the resultant signal are estimated using the proposed method.

TABLE III
PARAMETERS OF $x(t)$ FOR CASE STUDY 2

A_1	f_1 (Hz)	ζ_1	A_s	f_{ss} (Hz)	ζ_1
10	1.22	–0.07	3	18.5	[–0.24, –0.05]

Figure 6(a) and (b) shows the estimation errors of frequency and damping factor when the damping factor of the SSO mode varies from –0.24 to –0.05. It is observed that the esti-

mation errors of the frequency and damping factor are very low. The maximum estimation errors of the frequency and damping factor are approximately 0.004% and 1.0%, respectively. These results indicate the robustness of the proposed method against damping factor variations.

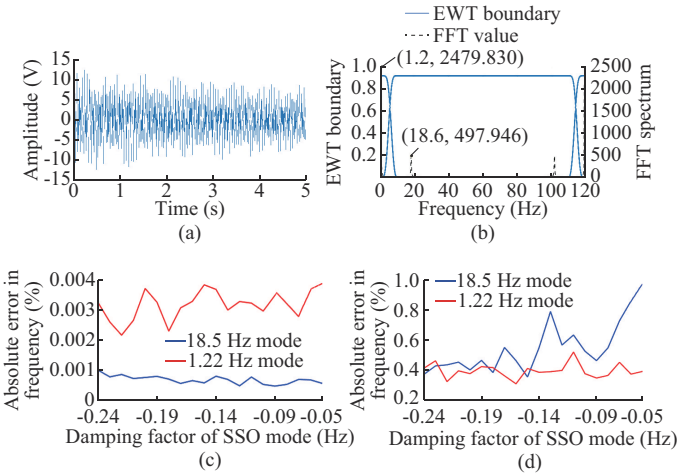

Fig. 6. Estimation error of parameters of $x(t)$ when damping factor of SSO mode varies from –0.24 to –0.05. (a) $x(t)$. (b) FFT of $x(t)$ with EWT boundaries. (c) Estimation error of frequency of $x(t)$. (d) Estimation error of damping factor of $x(t)$.

3) Case study 3: robustness against noise. In this case study, the performance of the proposed method against noise contamination is evaluated using $y(t)$. Figure 7 shows the estimation error of $y(t)$ when its SNR varies from 20 dB to 40 dB. It is noticed that the the estimation error of the frequency is negligible irrespective of the noise contamination of $y(t)$. However, the damping factor estimate of $y(t)$ obtained using the proposed method is slightly inaccurate at SNRs below 24 dB. However, at higher SNRs, the estimation error of damping factor is very low. For instance, the estimation error of the damping factor at 40 dB SNR is approximately 1%. Hence, it can be concluded that the proposed EWT-Yoshida method provides accurate parameter estimates irrespective of the noise contamination of the signal.

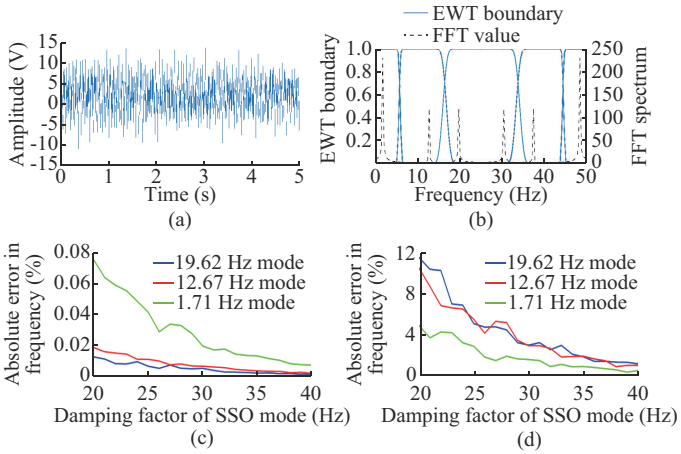

Fig. 7. Estimation error of $y(t)$ when its SNR varies from 20 dB to 40 dB. (a) $y(t)$ at 20 dB. (b) FFT of $y(t)$ with EWT boundaries. (c) Estimation error of frequency of $y(t)$. (d) Estimation error of damping factor of $y(t)$.

4) Case study 4: comparison with other methods. The accuracy of the parameter estimation of the proposed method is analyzed by comparing it with two other methods in this case study. Table IV shows the estimated values of $y(t)$ at different SNRs obtained through the proposed, VMD-Hilbert [17], and Prony-based [23] methods.

TABLE IV
ESTIMATED PARAMETERS OF $y(t)$ WITH DIFFERENT METHODS

SNR (dB)	Proposed method				VMD-Hilbert method [17]				Prony-based method [23]			
	f_i	ζ_i	Error in f_i (%)	Error in ζ_i (%)	f_i	ζ_i	Error in f_i (%)	Error in ζ_i (%)	f_i	ζ_i	Error in f_i (%)	Error in ζ_i (%)
25	19.6187	–0.1320	0.6500	5.6942	19.6177	–0.12010	0.0117	14.2620	19.6189	–0.1249	0.0060	10.79
	12.6687	–0.1431	1.0400	4.5821	12.6677	–0.01214	0.0180	19.0975	12.6706	–0.1468	0.0030	2.13
	1.7093	–0.1557	4.1400	2.7028	1.7097	–0.15540	0.0158	2.8597	1.7102	–0.1670	0.0010	4.38
30	19.6183	–0.1354	0.0035	3.2630	19.6183	–0.12330	0.0087	11.9482	19.6203	–0.1327	0.0015	5.27
	12.6691	–0.1453	0.0068	3.1162	12.6695	–0.14320	0.0040	4.5630	12.6697	–0.1459	0.0023	2.73
	1.7097	–0.1575	0.0184	1.5714	1.7099	–0.15080	0.0040	5.7503	1.7095	–0.1665	0.0294	4.06
35	19.6195	–0.1371	0.0026	2.0382	19.6200	–0.13260	0.0002	5.2762	19.6201	–0.1361	0.0005	2.79
	12.6696	–0.1476	0.0031	1.6273	19.6694	–0.14800	0.0050	1.3190	12.6703	–0.1463	0.0020	2.47
	1.7098	–0.1583	0.0109	1.0423	1.7091	–0.15190	0.0515	5.0850	1.7096	–0.1620	0.0234	1.25

It is noticed that all the methods provide good estimates of the frequency of modes. However, while estimating the damping factor of $y(t)$, the estimation error is the highest for the VMD-Hilbert method followed by the Prony-based method. In contrast, the estimation error is comparatively lower for the proposed method. The maximum estimation errors of damping factors in the proposed, Prony-based and VMD-Hilbert methods are approximately 5.69%, 10.79%, and 19.09%, respectively. At $SNR = 25$ dB, the estimation error in the proposed method is much smaller than that in the Prony-based and VMD-Hilbert methods. Hence, it can be inferred that the proposed method is more accurate than the Prony-based and VMD-Hilbert methods for SNRs above 25 dB.

B. Simulated and Actual SSO Signal [25]

The performance evaluation of the proposed method is further tested using simulated and actual SSO signal from the Hami Power Grid in Northwest China [25], [26].

1) Simulated SSO signal: the performance of the proposed method is tested using a simulated SSO signal in this case study. The simulated SSO signal used in this case study is shown in Fig. 8(a) and the simulation results of the proposed method are tabulated in Table V. The estimated parameters of simulated SSO signal at different noise levels are listed in Table VI.

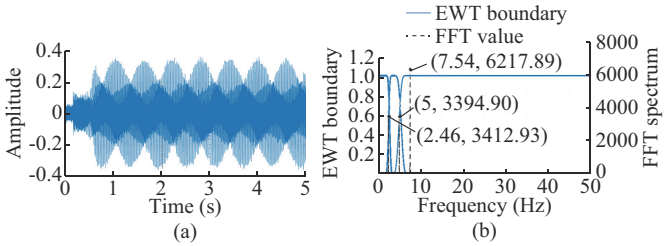

Fig. 8. PMU data of simulated SSO signal and its FFT plot. (a) PMU data corresponding to simulated SSO signal. (b) FFT plot of simulated SSO signal with EWT boundaries.

TABLE V
ESTIMATED PARAMETERS OF SIMULATED SSO SIGNAL USING DIFFERENT METHODS

Reported values [25]		Proposed method		VMD-Hilbert method [17]		Prony-based method [23]	
f_i (Hz)	ζ_i	f_i (Hz)	ζ_i	f_i (Hz)	ζ_i	f_i (Hz)	ζ_i
7.5125		7.5426	0.0009	7.7801	1.2319	8.0079	0.7128
		5.0001	0.0444	5.0095	1.2967		
		2.4573	0.8148				

TABLE VI
ESTIMATED PARAMETERS OF SIMULATED SSO SIGNAL AT DIFFERENT NOISE LEVELS

SNR (20 dB)		SNR (25 dB)		SNR (30 dB)		SNR (35 dB)	
f_i (Hz)	ζ_i	f_i (Hz)	ζ_i	f_i (Hz)	ζ_i	f_i (Hz)	ζ_i
7.5427	0.00072	7.5426	0.0009	7.5426	0.00085	7.5426	0.00091
5.0000	0.00027	5.0001	0.0004	5.0000	0.00036	5.0001	0.00038
2.4574	0.00072	2.4573	0.8148	2.4574	0.00074	2.4573	0.00081

It is observed from Table V that the proposed method identifies three modes with frequencies of 7.5426, 5.0001, and 2.4573 Hz from the simulated SSO signal. The FFT plot of this signal in Fig. 8(b) confirms the presence of these three modes with varying damping factors. Among these three modes, the 7.5426 Hz mode is the most dominant one as evident from its amplitude in the FFT plot. This value is similar to the reported one of the dominant SSO mode in [25]. However, it is noticed that the VMD-Hilbert and Prony-based methods only identify two modes and one mode, respectively. Furthermore, it is also observed that the estimated modal parameters of the 7.54 Hz mode through VMD-Hilbert and Prony-based methods are not accurate in comparison to the proposed method. Hence, it can be concluded that, the proposed EWT-Yoshida method is better suited for identifying and analyzing simulated SSO signals in comparison to other methods.

2) PMU data from actual SSO event: the performance of the proposed method is further tested using the PMU data corresponding to a real SSO event in the Hami Power Grid in Northwest China [25], [26], which has a high penetration of wind generators. The schematic representation of this data is shown in Fig. 9(a) from which a windowed signal having a length of 2 s is created, as shown in the figure. The analysis of this windowed signal is conducted using the proposed method and the results are tabulated in Table VII.

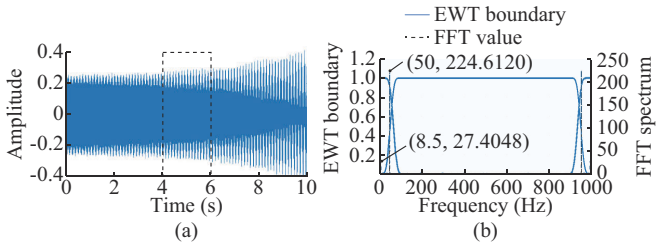

Fig. 9. PMU data from actual SSO event and its FFT plot. (a) PMU data corresponding to actual SSO event. (b) FFT plot of actual SSO signal with EWT boundaries.

TABLE VII
ESTIMATED PARAMETERS OF ACTUAL SSO SIGNAL USING DIFFERENT METHODS

Reported values [25]		Proposed method		VMD-Hilbert method [17]		Prony-based method [23]	
f_i (Hz)	ζ_i	f_i (Hz)	ζ_i	f_i (Hz)	ζ_i	f_i (Hz)	ζ_i
8.2871		8.2765	0.2287	8.9152	0.1913	8.7050	0.1962

It is observed from Table VII that the frequency of the dominant mode corresponding to the SSO event is found to be 8.2871 Hz. The results are similar to the reported values in the [25]. The FFT plot of the actual SSO signal also shows a mode with a frequency of 8.5 Hz, as shown in Fig. 9(b). It is also noticed that the estimated parameters of VMD-Hilbert and Prony-based methods are less accurate than the proposed method. Further, the estimates of the proposed method are almost constant irrespective of the noise contamination of the signal, as evident from Table VIII. Hence, it can be inferred from Tables VII and VIII that the proposed method effectively identifies and estimates SSO irrespective of the noise contamination of the signal.

TABLE VIII
ESTIMATED PARAMETERS OF ACTUAL SSO SIGNAL AT DIFFERENT NOISE LEVELS

SNR (20 dB)		SNR (25 dB)		SNR (30 dB)		SNR (35 dB)	
f_i (Hz)	ζ_i	f_i (Hz)	ζ_i	f_i (Hz)	ζ_i	f_i (Hz)	ζ_i
8.2782	0.2279	8.2740	0.2269	8.2763	0.2267	8.2763	0.2268

IV. CONCLUSION

EWT-based method for the analysis of SSO is proposed in this paper. The proposed method uses a preprocessing algorithm based on the WPSD estimate to identify the presence of SSO in the signal under consideration. If the presence of

SSO is confirmed, the signal is decomposed using the EWT, and the frequency and damping factor of the decomposed components are estimated using the Yoshida algorithm. The proposed method does not require any prior information about the signal unlike model based methods such as ESPRIT or other wavelet transform based methods. The performance of the proposed method is tested using test signals and actual SSO signal from the Hami Power Grid in Northwest China. The results reveal the effectiveness of the proposed method in detecting the SSO and estimating its parameters.

REFERENCES

[1] IEEE SSR Working Group and Others, "Reader's guide to subsynchronous resonance," *IEEE Transactions on Power Systems*, vol. 7, no. 1, pp. 150-157, Aug. 1992.

[2] J. Adams, C. Carter, and S. H. Huang, "ERCOT experience with subsynchronous control interaction and proposed remediation," in *Proceedings of PES T&D*, Orlando, USA, May 2012, pp. 1-5.

[3] J. Shair, X. Xie, L. Wang *et al*., "Overview of emerging subsynchronous oscillations in practical wind power systems," *Renewable and Sustainable Energy Reviews*, vol. 99, pp. 159-168, Jan. 2019.

[4] X. Xie, X. Zhang, H. Liu *et al*., "Characteristic analysis of subsynchronous resonance in practical wind farms connected to series-compensated transmissions," *IEEE Transactions on Energy Conversion*, vol. 32, no. 3, pp. 1117-1126, Sept. 2017.

[5] J. Fuentes-Velazquez, E. Beltran, E. Barocio *et al*., "A fast automatic detection and classification of voltage magnitude anomalies in distribution network systems using PMU data," *Measurement*, vol. 192, p. 110816, Mar. 2022.

[6] M. Q. Khan, M. M. Ahmed, and A. M. A. Haidar, "An accurate algorithm of PMU-based wide area measurements for fault detection using positive-sequence voltage and unwrapped dynamic angles," *Measurement*, vol. 192, p. 110906, Mar. 2022.

[7] K. M. El-Naggar, "On-line measurement of low-frequency oscillations in power systems," *Measurement*, vol. 42, no. 5, pp. 716-721, Jun. 2009.

[8] Y. Ma, Q. Huang, Z. Zhang *et al*., "Application of multisynchrosqueezing transform for subsynchronous oscillation detection using PMU data," *IEEE Transactions on Industry Applications*, vol. 57, no. 3, pp. 2006-2013, May 2021.

[9] R. Roy and T. Kailath, "ESPRIT-estimation of signal parameters via rotational invariance techniques," *IEEE Transactions on Acoustics, Speech, and Signal Processing*, vol. 37, no. 7, pp. 984-995, Jul. 1989.

[10] S. K. Jain and S. N. Singh, "Exact model order ESPRIT technique for harmonics and interharmonics estimation," *IEEE Transactions on Instrumentation and Measurement*, vol. 61, no. 7, pp. 1915-1923, Jul. 2012.

[11] C. Zhang, Z. Chen, M. Wang *et al*., "A novel identification method of power system oscillation based on dynamic mode decomposition," in *Proceedings of 2021 Power System and Green Energy Conference (PSGEC)*, Shanghai, China, Aug. 2021, pp. 713-717.

[12] Y. Wang, X. Jiang, X. Xie *et al*., "Identifying sources of subsynchronous resonance using wide-area phasor measurements," *IEEE Transactions on Power Delivery*, vol. 36, no. 5, pp. 3242-3254, Oct. 2021.

[13] X. Yang, J. Zhang, X. Xie *et al*., "Interpolated DFT-based identification of sub-synchronous oscillation parameters using synchrophasor data," *IEEE Transactions on Smart Grid*, vol. 11, no. 3, pp. 2662-2675, May 2020.

[14] D. Cai, Y. Ma, Z. Zhang *et al*., "Estimation of subsynchronous oscillation using a sliding window iterative DFT algorithm," in *Proceedings of 2021 3rd Asia Energy and Electrical Engineering Symposium (AEEES)*, Chengdu, China, Mar. 2021, pp. 337-340.

[15] K. Duda, L. B. Magalas, M. Majewski *et al*., "DFT-based estimation of damped oscillation parameters in low-frequency mechanical spectroscopy," *IEEE Transactions on Instrumentation and Measurement*, vol. 60, no. 11, pp. 3608-3618, Nov. 2011.

[16] S. Lin, F. Liu, and A. Dreglea, "Mode identification of broad-band oscillation signal based on improved VMD method," in *Proceedings of 2020 39th Chinese Control Conference (CCC)*, Shenyang, China, Jul. 2020, pp. 6162-6167.

[17] M. R. A. Paternina, R. K. Tripathy, A. Zamora-Mendez *et al*., "Identification of electromechanical oscillatory modes based on variational mode decomposition," *Electric Power Systems Research*, vol. 167, pp. 71-85, Feb. 2019.

[18] L. Chen, W. Zhao, F. Wang *et al*., "An interharmonic phasor and frequency estimator for subsynchronous oscillation identification and monitoring," *IEEE Transactions on Instrumentation and Measurement*, vol. 68, no. 6, pp. 1714-1723, Jun. 2019.

[19] J. Gilles, "Empirical wavelet transform," *IEEE Transactions on Signal Processing*, vol. 61, no. 16, pp. 3999-4010, Aug. 2013.

[20] I. Yoshida, T. Sugai, S. Tani *et al*., "Automation of internal friction measurement apparatus of inverted torsion pendulum type," *Journal of Physics E*: *Scientific Instruments*, vol. 14, no. 10, pp. 1201-1206, Oct. 1981.

[21] J. G. Philip, Y. Yang, and J. Jung, "Identification of power system oscillation modes using empirical wavelet transform and Yoshida-Bertecco algorithm," *IEEE Access*, vol. 10, pp. 48927-48935, Oct. 2022.

[22] J. Shair, X. Xie, L. Yuan *et al*., "Monitoring of subsynchronous oscillation in a series-compensated wind power system using an adaptive extended Kalman filter," *IET Renewable Power Generation*, vol. 14, no. 19, pp. 4193-4203, Dec. 2020.

[23] D. P. Wadduwage, U. D. Annakkage, and K. Narendra, "Identification of dominant low-frequency modes in ring-down oscillations using multiple Prony models," *IET Generation*, *Transmission & Distribution*, vol. 9, no. 15, pp. 2206-2214, Nov. 2015.

[24] O. M. Jr. Solomon. (1991, Dec.). PSD computations using Welch's method. [Online]. Available: https://www.osti.gov/biblio/5688766

[25] F. Zhang, J. Li, J. Liu *et al*., "An improved interpolated DFT-based parameter identification for sub-/super-synchronous oscillations with synchrophasors," *IEEE Transactions on Power Systems*, vol. 38, no. 2, pp. 1714-1727, Mar. 2023.

[26] IEEE Dataport. (2022, Nov.). PMU data for actual SSO event. [Online]. Available: https://ieee-dataport. org/openaccess/simulated-synchrophasors-ssos-and-phasor-measurement-datarecorded-during-subsynchronous

Joice G. Philip received the M.Tech degree in power system from National Institute of Technology, Calicut, India, in 2013, and the Ph. D. degree in electrical engineering from Indian Institute of Technology (IIT), Indore, India, in 2019. Since August 2021, he has been a Postdoctoral Fellow with the Department of Energy Systems Research, Ajou University, Suwon City, South Korea. His research interests include power system stability, phasor measurement units and distributed energy resource management system.

Jaesung Jung received the B.S. degree in electrical engineering from Chungnam National University, Daejeon, Korea, the M.S. degree in electrical engineering from the North Carolina State University, Raleigh, USA, and the Ph. D. degree in electrical engineering from the Virginia Tech, Blacksburg, USA. He is currently a Faculty Member in the Department of Energy Systems Research at Ajou University, Suwon City, Korea. His research interests include development and deployment of renewable and sustainable energy technologies.

Ahmet Onen received the B. Sc. degree in electrical-electronic engineering from Gaziantep University, Gaziantep, Turkey, in 2005, the M. S. degree in electrical-computer engineering from Clemson University, Clemson, USA, in 2010, and the Ph. D. degree in Electrical and Computer Engineering Department from Virginia Tech, Blacksburg, USA, in 2014. He is currently working as an Associate Professor in Sultan Qaboos University, Muscat, Oman. His research interests include smart grid and sustainable energy technologies.